Orientation Analysis of ω-Substituted Long-Chain Alkanethiols Self-Assembled on Au Substrate

ARTICLE *in* THE JOURNAL OF PHYSICAL CHEMISTRY C · OCTOBER 2008

Impact Factor: 4.77 · DOI: 10.1021/jp8069282

4 AUTHORS, INCLUDING:

Polina Angelova
CNM Technologies GmbH
13 PUBLICATIONS **75** CITATIONS
SEE PROFILE

D. Tsankov
Bulgarian Academy of Sciences
41 PUBLICATIONS **424** CITATIONS
SEE PROFILE

Orientation Analysis of ω-Substituted Long-Chain Alkanethiols Self-Assembled on Au Substrate

Polina N. Angelova,[†] Karsten Hinrichs,*[,‡] Kalina V. Kostova,[†] and Dimiter T. Tsankov*[,†]

Institute of Organic Chemistry, Bulgarian Academy of Sciences, Acad. G. Bonchev Street, Block 9, 1113 Sofia, Bulgaria, and ISAS - Institute for Analytical Sciences, Department Berlin, Albert-Einstein-Strasse 9, 12489 Berlin, Germany

Received: August 4, 2008; Revised Manuscript Received: September 9, 2008

Monolayers from *para*-substituted benzyl esters of 16-mercaptohexadecanoic acid (R = −Cl; $-OCH_3$) self-assembled on (111)-textured gold films have been studied in detail with infrared and visible spectroscopic ellipsometry and contact angles measurements. The experimental data testify that these monolayers on gold tend to adopt tilt angles smaller than typical for *n*-alkanethiols, while the orientation of the phenyl rings is almost perpendicular to the surface. The same precursor molecules self-assembled on silver showed arrangement of the aliphatic chains characteristic for long-chain alkanethiols but differently tilted orientation of the terminal phenyl rings. An attempt was made to explain that different behavior with the different surface energetics of gold and silver substrates.

1. Introduction

Self-assembled monolayers (SAMs) of *n*-alkanethiols on metallic surfaces have been the subject of intensive studies for more than two decades.[1−3] The possibility to tailor physical and chemical properties of a surface by choosing suitably modified SAMs opens new areas for diverse applications of nanoscale-based materials. Growing attention has been recently focused on functionalized SAMs because of their potential application for fabrication of molecular electronic components and nanostructure-based devices.[4−7] An important attribute of SAMs formed by functionalized alkanethiols is the structure of and the orientation within these films. It is intuitively assumed that the packing and orientation of the carbon chains would be similar to or even the same as in the overlayers formed by the parent *n*-alkanethiols. Incorporation of different chemical functionalities as well as aromatic terminal substituents aiming to modify the outermost film properties may also introduce different orientation order within the monolayers as a result of minimizing the unfavorable intermolecular interactions of the adjacent chains.[2,3,8−11]

In a preceding study we examined the film structure of some *para*-substituted benzyl esters of 16-mercaptohexadecanoic acid self-assembled on silver substrates (R = −Cl; $-OCH_3$; $-NO_2$; −CN).[12] The IR ellipsometric data indicated almost upright position of the carbon chains, and, similarly to *n*-alkanethiols, they are characterized by small tilt angles in the vicinity of 10°. The water advancing contact angles were clustered in tight intervals irrespective of the different polar character of the end groups. The data indicated wetting considerably lower than that typical for *n*-alkanethiols with end polar groups such as $-OCH_3$ and −CN,[13] and closer to monolayers formed by aryl-terminated alkanethiols.[11] Careful inspection of the IR ellipsometric data revealed specific orientation of the phenyl rings, which adopt a lamellar structure and remain closely exposed to the interface.[12] Unexpectedly, the same monolayers on gold demonstrated different ordering in both the carbon chains and the tale terminus. Such various molecular arrangements on different metallic substrates might have a significant impact on the functional properties of these films such as wetting or lateral conductivity.

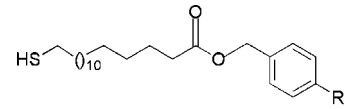

1 R = Cl

2 R = OCH_3

Figure 1. Chemical structure of the model compounds.

As a part of a larger project aiming to ascertain the electronic and the steric influence on the organizational order of SAMs formed by tailored alkanethiols and to survey their behavior on different metallic substrates, we report here on the structure and orientation of SAMs formed by *para*-substituted benzyl esters of 16-mercaptohexadecanoic acid on gold. SAMs formed by molecules of similar kind have been reported to show notable anisotropic conductivity on Si.[14]

2. Materials and Methods

The synthesis of model compounds **1** and **2** (Figure 1) has been published previously.[15] Gold substrates (200 nm gold with a titanium intermediate layer on glass) were purchased from Ssens (The Netherlands). Spectroscopy-grade methylene chloride was obtained from Merck and used as received. Glassware was cleaned with piranha solution (30% H_2O_2/98% H_2SO_4 = 3:7) for 30 min at 90 °C.

2.1. Monolayer Preparation. The gold substrates were first annealed for a few seconds on an acetylene burner (2300 °C) in order to remove possible organic contaminants and then immersed in a 10^{-3} M solution of the compound studied in CH_2Cl_2 (Merck) at room temperature overnight. Before the ellipsometric measurements, the samples were rigorously cleaned

* Corresponding author. E-mail: dtsankov@orgchm.bas.bg (D.T.T.); karsten.hinrichs@isas.de (K.H.).
† Bulgarian Academy of Sciences.
‡ Institute for Analytical Sciences.

10.1021/jp8069282 CCC: $40.75
Published on Web 10/21/2008

in pure solvent by ultrasonic bath for 10 min, rinsed thoroughly with methylene chloride, and blown dry with Ar. Such a procedure effectively removes the physisorbed molecules from the surface.

2.2. Infrared Ellipsometry. Infrared spectroscopic ellipsometry is an incisive tool for studying optical constants, thicknesses, and anisotropic properties of thin films on various substrates[16] (and the references therein). It has a potential to characterize the composition, structure, and thickness of the film in one measurement on a definite sampling area. The film optical constants n and k and thickness d are inferred from ellipsometric data by model calculations based on the classical electromagnetic wave theory. The calculated values are used further to simulate the experimental ellipsometric spectra. The results are compared, and the model is refined until the best fit is reached.[16,17]

The spectra were recorded by an IR ellipsometer described in detail elsewhere.[18] During the ellipsometric measurement, the sample is irradiated by linearly polarized radiation, and the reflected elliptically polarized beam is analyzed. The sample was placed on a goniometer at incidence angles of 65° and 70°. The spectra were recorded with a globar source and a mercury cadmium telluride (MCT) detector in the 4000−800 cm^{-1} range and at spectral resolution of 4 cm^{-1}.

A typical ellipsometric experiment includes a set of four single-beam measurements taken with the analyzer fixed at 45° in relation to the plane of incidence and the front polarizer consecutively set at 0° and 90° and then at 45° and 135°. The single-beam spectra were pairwise ratioed and converted further into the ellipsometric parameters tan Ψ and Δ.[18] The data collection typically included averaging of 24 cycles of measurements where 64 scans were coadded for each set. The whole measurement procedure was fully automated using Opus Macro software (Bruker).

2.3. VIS Ellipsometry. The VIS ellipsometric measurements were performed by variable angle spectroscopic ellipsometer SE-801-E, SENTECH GmbH, Germany. The thicknesses were determined from a best-fit on three angle measurements at 60°, 65°, and 70° in the spectral range of 400−700 nm.

2.4. Contact Angles. Water advancing contact angles were measured with the captive drop method under ambient conditions. The contact angle values were averages of three measurements at different locations.

2.5. Calculations. The calculation procedure applied was based on the classical three-phase model to determine the film optical constants and thickness. The mathematical algorithm follows the model proposed by Azzam and Bashara,[19] which accounts for the anisotropic properties of the film optical constants and therefore affords calculating the band intensities as a function of molecular orientation. An optical layer calculation was applied to simulate the measured ellipsometric spectra. The following parameters of the oscillator strengths[20] F_z were used: 8200 cm^{-2} for $\nu_{as}(CH_2)$, 3360 cm^{-2} for $\nu_s(CH_2)$, and 4100 cm^{-2} for ν (CC) of the phenyl ring. The parameter of the oscillator strength (F) was introduced for the wavenumber-dependent form of the dielectric function in the Lorentz oscillator model (see, e.g., ref 20). This parameter F can be transformed into a dimensionless oscillator strength S (as defined in ref 21) by division by the square of the oscillator position in wavenumbers (σ_0^2).

3. Results and Discussion

3.1. Contact Angles. The water advancing contact angles for SAMs formed by molecules **1** and **2** on gold substrates are listed in Table 1 together with their respective values on silver substrates. For comparison, the contact angles of −Cl- and $-OCH_3$-terminated long-chain n-alkanethiols on gold[13] are also given, because they characterize the hydrophilic character of SAMs whose outer shells are formed entirely by these groups. Their values (83° for −Cl, and 74° for $-OCH_3$) are rather lower than the 110° found for the methyl-terminated n-alkanethiols,[13] which is attributed to the recognized polar character of these groups. The contact angles for SAMs of **1** and **2** on silver substrates are clustered in a very tight interval (90−87°), and their values suggest wetting distinctly lower than this for the corresponding −Cl- and $-OCH_3$-terminated long-chain n-alkanethiols. This behavior was attributed to a specific conformation of the tale terminus in which the phenyl rings adopt tilted lamellar orientation.[12] This orientation effectively minimizes the influence of the end groups and results in contact angle values typical for monolayers formed from aryl-terminated n-alkanethiols.[11]

TABLE 1: Water Advancing Contact Angles for the Model Compounds 1 and 2 and Reference Data for Analogously Substituted *n*-Alkanethiols

	substrates		substituted n-alkanethiols
model compounds	Au	Ag[a]	Au[b]
1 Cl	58°	90°	83°
2 OCH_3	64°	87°	74°

[a] Data taken from ref 12. [b] Data taken from ref 13.

The water advancing contact angles for SAMs of **1** and **2** on gold substrates are substantially lower than those for the same SAMs on silver as well as from the corresponding −Cl- and $-OCH_3$-terminated n-alkanethiols on gold. The reduced values of the contact angles suggest an added hydrophilic character. This contribution may solely arise from the low-lying oxygen atoms of the carbonyl and the ester groups, which can interact with water molecules. Such an interaction was not possible for the SAMs on silver because of specific lamellar orientation of the phenyl rings at the interface, which shield the low-lying oxygen atoms. Different orientation of the phenyl rings is required to facilitate the interaction of water molecules with oxygen atoms of the carbonyl and the ester groups.

3.2. VIS and IR Ellipsometry. VIS and IR ellipsometric measurements were simulated to evaluate the optical constants, thicknesses and orientation of the monolayers. Uniaxial symmetry was assumed for all simulations. Optical constants of the substrate have been determined from independent measurement of an annealed blank Au substrate. The evaluation of the SAM thickness was done by VIS ellipsometry and fitting in the three-phase model. Assuming a value of 1.4 for n_∞ of the monolayer and neglecting any possible anisotropy, the simulations resulted in a thickness of 2.9 nm for film **1** and 3.1 nm for film **2**. Such best-fit simulations do not account for the interfacial layer between the substrate and the SAM. More demanded model calculations may include surface and interface roughness.[22,23] Recent calculations within the effective medium approximation (EMA)[24] performed for VIS ellipsometry measurements of 1-octadecanethiol monolayers on gold estimated an interfacial layer in the vicinity of 0.3−0.4 nm.[25]

3.2.1. SAM Organizational Structure: The Aliphatic Chains. The orientation of the polymethylene chains and the terminal phenyl rings can be probed by IR reflection−absorption spectroscopy or IR spectroscopic ellipsometry. The latter is sometimes more advantageous because the ellipsometric spectra tan Ψ and Δ are absolute measures, and they can be simulated

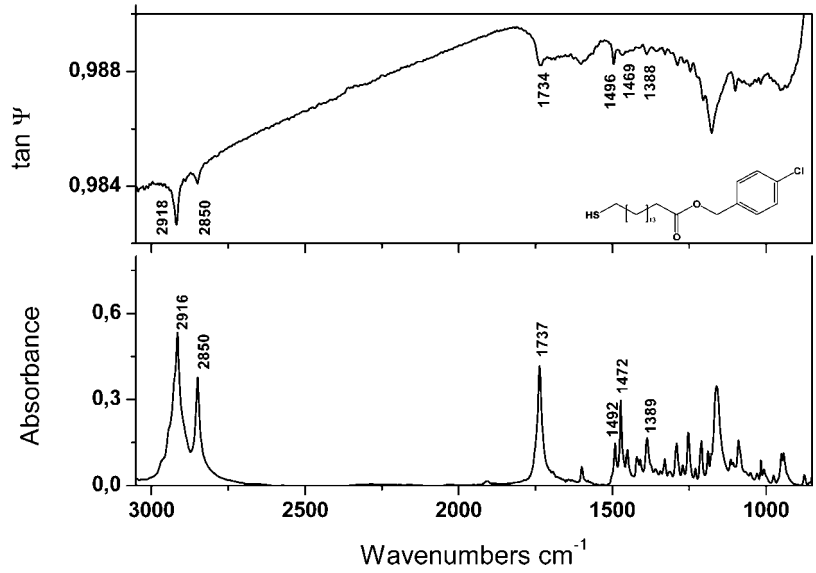

Figure 2. (Top) tan Ψ ellipsometric spectrum of 4-chlorobenzyl 16-mercaptohexadecanoate (**1**) monolayer on Au(111), measured at an angle of incidence of 70° and a resolution of 4 cm^{-1}. (Bottom) IR absorption in KBr. All IR absorption spectra are measured at a sample concentration of 1 mg/300 mg KBr.

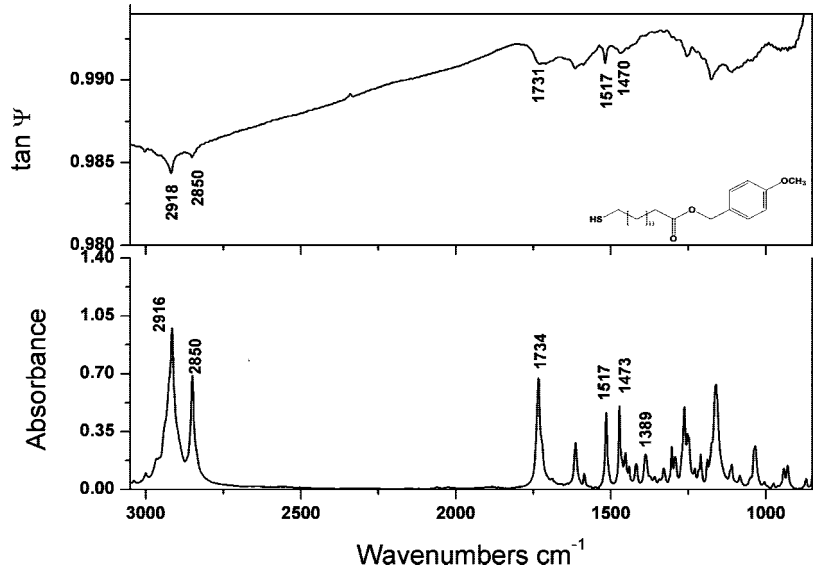

Figure 3. (Top) 4-Methoxybenzyl 16-mercaptohexadecanoate (**2**) monolayer self-assembled on Au(111) substrate. tan Ψ spectrum measured at an incidence angle of 70°. (Bottom) IR absorption in KBr.

quantitatively with respect to the complex optical constants, thickness, and molecular orientation.[16] While the various tan Ψ band shapes of thin films on nonmetallic surfaces are direct characteristics for the molecular orientation,[16] the vibrational bands of thin organic films on metallic substrates have simple "transmission-like" shape owing to the *surface selection rule*.[26] By the same token, the molecular orientation is inferred from the amplitudes of selected vibrational modes whose transition moments are differently projected onto the surface normal. The amplitude tan Ψ spectra of compounds **1** and **2** are presented in Figures 2 and 3 together with the corresponding IR absorption spectra in solid state. Peak frequencies of some characteristic IR bands taken from the ellipsometric spectra as well as measured in KBr pellets along with mode assignments are listed in Table 2.

The bands corresponding to the antisymmetric methylene stretching $\nu_{as}(CH_2)$ of both SAMs are located at 2918 cm^{-1}. This wavenumber is very close to the IR absorption in the polycrystalline state (2916 cm^{-1}) and indicates the alkyl chains are well packed, fully extended, and mostly exist in all-trans conformation, characteristic for hydrocarbons in the crystalline state.[29] A comparison of the observed band shapes also shows negligible differences, further indicating similar conformations of the chains in crystalline and monolayer phases. Progressive band structure, well pronounced for the absorptions in the 1350−1150 cm^{-1} region is also detectable in tan Ψ spectra. Depicted by very weak features, better discernible for **1**, it also testifies for a crystalline-like environment. It consists of a series of coupled twisting and wagging CH_2 modes that arise when all-trans conformation exists along the backbone of long-chain hydrocarbons.[30] Judging by the altered relative intensity ratio of the two methylene stretching modes during the transition from polycrystalline state to ordered film (Figures 2 and 3) and accounting for the surface selection rule, one can infer that the chains are tilted with respect to the surface normal. Another clue is the substantial intensity reduction of the $\delta(CH_2)$ scissoring deformation band in tan Ψ spectra, implying that its transition dipole moment is nearly parallel to the surface.

TABLE 2: Most Prominent Observed Frequencies for Compounds 1 and 2

compound	tan Ψ (film) (cm^{-1})	KBr (cm^{-1})	assignment[a]
1	2918	2916	$\nu_{as}(CH_2)$
	2850	2850	$\nu_s(CH_2)$
	1734	1737	$\nu(C{=}O)$
	1496	1492	$\nu(CC)_{Ar}$ 19a[b]
	1469	1472	$\delta(CH_2)$
	1388	1389	$\nu(CC)_{Ar}$ 19b[b]
2	2918	2916	$\nu_{as}(CH_2)$
	2850	2850	$\nu_s(CH_2)$
	1731	1734	$\nu(C{=}O)$
	1517	1517	$\nu(CC)_{Ar}$ 19a[b]
	1470	1473	$\delta(CH_2)$
	–	1389	$\nu(CC)_{Ar}$ 19b[b]

[a] Assignments as described in the literature.[27,28] [b] Notations for phenyl vibrations as introduced by Wilson and commonly adopted in the literature.[28]

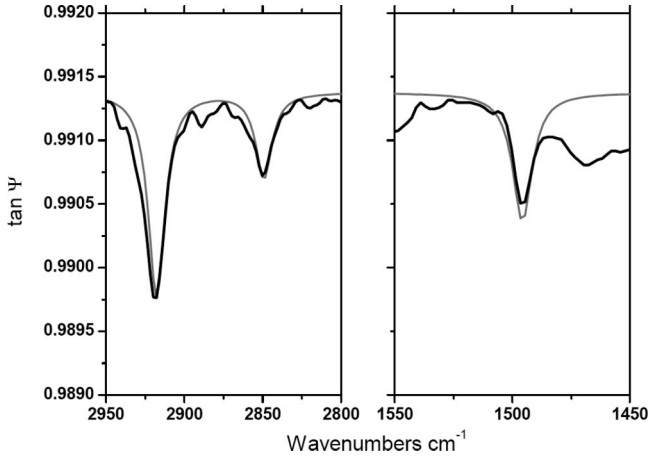

Figure 4. Simulated (gray line) and experimental (black line) fragments of the tan Ψ spectrum of 4-chlorobenzyl 16-mercaptohexadecanoate on Au(111). The following parameters have been used for the calculations: $n_\infty = 1.4$, the parameters of the oscillator strengths F_z are as follows: 8200 cm^{-2} for $\nu_{as}(CH_2)$, 3360 cm^{-2} for $\nu_s(CH_2)$, and 4100 cm^{-2} for ν(CC) of the phenyl ring.

The tilt angle of the polymethylene chains was determined using two independent methods proposed by Debe[31] and Parikh and Allara.[32] Both calculation approaches affirmed conformable results: $9 \pm 1°$ from the spectral simulations and $11 \pm 2°$ from the method of Debe. The twist angles defined by the CCC plane of the chain axis and the plane established by the vectors of the chain axes and the surface normal were in the range of 55−60° for both methods. Figure 4 depicts the optical simulation of the tan Ψ spectrum for molecule **1** on gold.

The tilts calculated for **1** and **2** on Au (111) surfaces are very close to the values found for the same molecules on Ag substrates.[12] While distinctive for *n*-alkanethiols on Ag, the tilt angles differ from that commonly reported for Au (111)[1−3,29] and are much closer to these observed on Au(100) crystallographic texture.[33] It is generally accepted that the bonding of thiols on Au(111) is based on a hexagonal overlayer ($\sqrt{3} \times \sqrt{3}$)$R30°$.[1−3] Evidence for deviation from pure hexagonal symmetry and the existence of a secondary ordering of the carbon chains corresponding to a $c(4 \times 2)$ superlattice was observed by IR,[33] scanning tunneling microscopy (STM),[34,35] and low-energy atom diffraction (LEAD).[36,37] The two-dimensional arrangement in SAMs is determined by two factors: the bonding sites of the sulfur moieties (3-fold hollow and bridge sites) and the lateral interactions of the adjacent chains. In order to minimize the surface free energy, the molecules are forced to such conformations that would effectively increase the favorable van der Waals interactions.[2,3] In the case of terminal voluminous substituents, a secondary lateral organizational order may emerge that would change the macroscopic physical-chemical properties of the monolayer, such as wetting. These interactions could also change the orientations of the aliphatic chains. For cases where the steric constraints of the neighboring molecules prevent the ordering typical for *n*-alkanethiols, other two-dimensional organization of the monolayer is observed.[3] Most typical examples are SAMs composed of *p*-substituted biphenylthiols and terphenylthiols, where the tilt angles found on Ag(111) and Au(111) are almost equal.[38−40]

3.2.2. SAM Organizational Structure: The Aryl Substituents. The water advancing contact angles indicated increased hydrophilic character of the outer SAM surface on gold. The values are substantially lower than these of the analogous SAMs on Ag and remain distinctly less than those composed by aliphatic chains with polar end groups. The data suggest increased hydrophilic character of these SAMs in comparison with their analogues on Ag. This enhancement could only arise from interaction of water molecules with other polar groups. Groups such as ester and carbonyl groups are available for interaction provided that the phenyl rings could adopt a specific orientation that would reduce the shielding and would alleviate the access of water molecules. The flexible CH_2 linkage of the benzyl group facilitates the free rotation around the C−Ph bond and allows change of the phenyl ring orientation. Suitable probes for aromatic ring orientation are the aromatic modes 19a and 19b, according to Wilson notation commonly adopted in the literature.[27,28] The transition dipole moments of 19a and 19b modes in 1,4-disubstituted benzene derivatives are mutually orthogonal, as 19a mode is polarized along the direction of both substituents.[28] Owing to the surface selection rule in the infrared spectral range for thin organic films on metallic surfaces, only those vibrations that have transition dipole moment components in the direction of the surface normal are detectable. The comparison of the relative IR intensities of these modes in solid state, where the molecules are randomly oriented, and in the film where the molecules are ordered, allows one to qualitatively infer the relative orientation of the phenyl rings. Referring to Figure 2, the absorptions of 19a and 19b located at 1492 and 1389 cm^{-1}, respectively, show almost equal intensities, as the intensity of 19b is slightly higher. An entirely different intensity distribution is observed in the tan Ψ spectrum of the monolayer. Manifold increased intensity is observed for 19a in comparison to 19b that is related to the larger projection of this dipole transition moment on the surface normal. The intensities of 19a and 19b in **2** are changed even to a larger extent upon transition from randomly oriented molecules dispersed in KBr to ordered film (Figure 3). The band located at 1517 cm^{-1}, which is associated with the 19a mode, appears to be one of the most prominent bands in the tan Ψ spectrum, while the band at 1389 cm^{-1} corresponding to the 19b mode is hardly discernible. This is also sound evidence for the changed orientation of the phenyl rings, which tend to stand almost perpendicular to the surface. The conceivable orientation of molecules **1** and **2** self-assembled on (111)-textured gold substrate is presented in Figure 5a. For comparison, the orientation of the same molecules on Ag(111), taken from ref 12 is shown in Figure 5b.

SAMs composed of identical molecules showed impressive organizational behavior on Au(111) and Ag(111) substrates. Although the nearest neighbor distances in the two lattices are almost equal (2.88 Å vs 2.89 Å, respectively), different

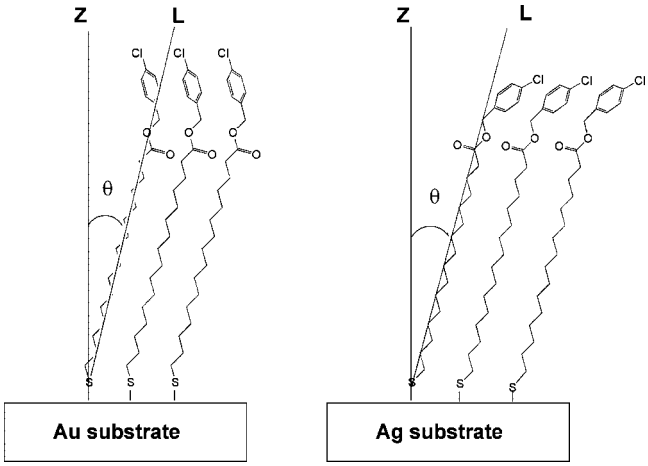

Figure 5. Conceivable phenyl ring orientation of SAMs (a) on gold and (b) on silver.[12] Z = surface normal; L = long molecular axis; θ = tilt angle with respect to the surface normal.

organizational patterns of thiolates are observed resulting in a $(\sqrt{3} \times \sqrt{3})R30°$ overlayer on Au(111) and a $(\sqrt{7} \times \sqrt{7})R10.9°$ overlayer on Ag(111).[41,42] The surfaces are energetically inhomogeneous, which determines the preferred bonding sites. While the typical bonding sites on gold are 3-fold hollow and bridge sites, adsorption at an on-top site and at a hollow site can occur on silver because of smoother binding energy surface.[43] Hence the same molecules bound on energetically different lattices may adopt different organizational behaviors.

Conclusions

Compounds **1**and **2** self-assemble onto (111)-textured gold surfaces to form densely packed and well-ordered monolayers. The IR ellipsometric data show that the hydrocarbon chains reside in crystalline-like environment and exist in predominantly all-trans conformation with low populations of gauche defects. The calculations carried out with two methods [31,32] proved small tilt angles: $9 \pm 1°$ and $11° \pm 2°$ for the hydrocarbon chains. Although these values are rather typical for Au(100) where SAMs are organized as a $c(2 \times 2)$ overlayer[31] compared to those for Au (111), such structural arrangements cannot be excluded from consideration when thiols with different steric requirements from that of *n*-alkanethiols are self-assembled.[38−40] The water advancing contact angles found for **1** and **2** indicate increased hydrophilic character from that already observed for the same SAMs on silver. This augmented wetting could occur provided that water molecules have access to the carbonyl and/or ester groups. Such contact was not possible for the SAMs on Ag because of the demonstrated shielding effect of the phenyl rings.[12] Evidently, different orientation of the end phenyl rings is required to admit the water molecules down to the oxygen atoms. The analysis based on the intensity ratio of the 19a and 19b modes in IR absorption and ellipsometric tan Ψ spectra suggested close to vertical arrangement of the aryl substituents. Such an arrangement provides enough space and direct access of water molecules to lower-lying oxygen atoms.

Acknowledgment. The authors are indebted to Prof. J. Petrov and Ms. T. Andreeva, Institute of Biophysics, Bulgarian Academy of Sciences, for the contact angle measurements and some fruitful discussions. Thanks are also due to Dr. C. Cobet and Prof. Dr. N. Esser, ISAS Berlin, for cooperation. The technical assistance of Ms I. Fisher, ISAS Berlin, is gratefully acknowledged. The financial support by the Deutsche Forschungsgemeinschaft and the Bulgarian Academy of Sciences (contract 436 BUL 113/127), the Senatsverwaltung für Wissenschaft, Forschung and Kultur des Landes Berlin, the Bundesministerium für Bildung, Wissenschaft, Forschung and Technologie is gratefully acknowledged.

References and Notes

(1) Dubois, L. H.; Nuzzo, R. G. *Annu. Rev. Phys. Chem.* **1992**, *43*, 437.
(2) Schreiber, F. *Prog. Surf. Sci.* **2000**, *65*, 151.
(3) Love, J. C.; Estroff, L. A.; Kriebel, J. K.; Nuzzo, R. G.; Whitesides, G. M. *Chem. Rev.* **2005**, *105*, 1103.
(4) Li, Z.; Chang, S. C.; Williams, R. S. *Langmuir* **2003**, *19*, 6744.
(5) Shi, D. X.; Ji, W.; Lin, X.; He, X. B.; Lian, J. C.; Gao, L.; Cai, J. M.; Lin, H.; Du, S. X.; Lin, F.; Seidel, C.; Chi, L. F.; Hofer, W. A.; Fuchs, H.; Gao, H.-J. *Phys. Rev. Lett.* **2006**, *96*, 226101.
(6) Akkerman, H. B.; Blom, P. W. M.; de Leeuw, D. M.; de Boer, B. *Nature* **2006**, *441*, 69.
(7) Maisch, S.; Buckel, F.; Effenberger, F. *J. Am. Chem. Soc.* **2005**, *127*, 17315.
(8) Fox, M. A.; Wooten, M. D. *Langmuir* **1997**, *13*, 7099.
(9) Wacker, D.; Weiss, K.; Kazmaier, U.; Wöll, Ch. *Langmuir* **1997**, *13*, 6689.
(10) Danneberger, O.; Weiss, K.; Himmel, H.-J.; Jäger, B.; Buck, M.; Wöll, Ch. *Thin Solid Films* **1997**, *307*, 183.
(11) Buckel, F.; Effenberger, F.; Yan, Ch.; Gölzhäuser, A.; Grunze, M. *Adv. Mater.* **2000**, *12*, 901.
(12) Angelova, P.; Hinrichs, K.; Esser, N.; Kostova, K.; Tsankov, D. *Vibr. Spectrosc.* **2007**, *45*, 55.
(13) Bain, C. D.; Troughton, E. B.; Tao, Y. T.; Evall, J.; Whitesides, G.; Nuzzo, R *J. Am. Chem. Soc.* **1989**, *111*, 321.
(14) Collet, J.; Lenfant, S.; Vuillaume, D.; Bouloussa, O.; Rondelez, F.; Gay, J. M.; Kham, K.; Chevrot, C. *Appl. Phys. Lett.* **2000**, *76*, 1339.
(15) Angelova, P.; Kostova, K.; Hinrichs, K.; Tsankov, D. *Cent. Eur. J. Chem.* **2005**, *3*, 658.
(16) Hinrichs, K.; Gensch, M.; Esser, N. *Appl. Spectrosc.* **2005**, *59*, 272A.
(17) Tsankov, D.; Hinrichs, K.; Korte, E. H.; Dietel, R.; Röseler, A. *Langmuir* **2002**, *18*, 6559.
(18) Röseler, A.; Korte, E. H. In *Handbook of Vibrational Spectroscopy*; Chalmers, J. M., Griffiths, P. R., Eds.; John Wiley & Sons, Ltd: Chichester, U.K., 2001; Vol. 2, p 1065.
(19) Azzam, R. M. A.; Bashara, N. M. *Ellipsometry and Polarized Light*; North-Holland Publishing Co.: Amsterdam, 1977.
(20) Röseler, A. In *Handbook of Ellipsometry*; Tompkins, H. G., Irene, E. A., Eds.; William Andrew, Inc: Springer, 2005; p 779.
(21) Tolstoy, V. P.; Chernyshova, I. P.; Skryshevsky, V. A. *Handbook of Infrared Spectroscopy of Ultrathin Films*; John Wiley & Sons, Inc.: Hoboken, NJ, 2003; p 20.
(22) Shi, J.; Hong, B.; Parikh, A. N.; Collins, R. W.; Allara, D. L. *Chem. Phys. Lett.* **1995**, *246*, 90.
(23) Mårtensson, J.; Arwin, H. *Langmuir* **1995**, *11*, 963.
(24) Bruggeman, D. A. G. *Ann. Phys.* **1935**, *416*, 665.
(25) Prato, M.; Moroni, R.; Bisio, F.; Rolandi, R.; Mattera, L.; Cavalleri, O.; Canepa, M. *J. Phys. Chem.* **2008**, *112*, 3899.
(26) Greenler, R. G. *J. Chem. Phys.* **1966**, *44*, 310.
(27) Roeges, N. P. G. *A Guide to the Complete Interpretation of Infrared Spectra of Organic Molecules*; Wiley: Chichester, U.K., 1994.
(28) Varsányi, G. *Vibrational Spectra of Benzene Derivatives*; Akadémiai Kiadó: Budapest, 1969; Chapter 3.
(29) Nuzzo, R. G.; Dubois, L. N.; Allara, D. *J. Am. Chem. Soc.* **1990**, *112*, 558.
(30) Snyder, R. G.; Schachtschneider, J. H. *Spectrochim. Acta* **1963**, *19*, 85.
(31) Debe, M. K. *J. Appl. Phys.* **1984**, *55*, 3354.
(32) Parikh, A. N.; Allara, D. L. *J. Chem. Phys.* **1992**, *96*, 927.
(33) Dubois, L. H.; Zegarski, B. R.; Nuzzo, R. G. *J. Chem. Phys.* **1993**, *98*, 678.
(34) Poirier, G. E. *Chem. Rev.* **1997**, *97*, 1117.
(35) Bucher, J. P.; Santesson, L.; Kern, K. *Appl. Phys. A: Mater. Sci. Process.* **1994**, *59*, 135.
(36) Nuzzo, R. G.; Korenic, E. M.; Dubois, L. H. *J. Chem. Phys.* **1990**, *93*, 767.
(37) Camillone, N.; Chidsey, C. E. D.; Liu, G.-Y.; Scoles, G. *J. Chem. Phys.* **1993**, *98*, 4234.
(38) Frey, S.; Stadler, V.; Heister, K.; Eck, W.; Zharnikov, M.; Grunze, M.; Zeysing, B.; Terfort, A. *Langmuir* **2001**, *17*, 2408.
(39) Duan, L; Garrett, S. J. *J. Phys. Chem. B* **2001**, *105*, 9812.
(40) Kang, J. F.; Ulman, A.; Liao, S.; Jordan, R.; Yang, G.; Liu, G.-Y. *Langmuir* **2001**, *17*, 95.
(41) Schwaha, K.; Spencer, N. D.; Lambert, R. M. *Surf. Sci.* **1979**, *81*, 273.
(42) Rovida, G.; Pratesi, F. *Surf. Sci.* **1981**, *104*, 609.
(43) Ulman, A. *Chem. Rev.* **1996**, *96*, 1533.

JP8069282